Influence of the Degree of Substitution on the Solution Properties of Chloromethylated Polysulfone

Silvia Ioan, Anca Filimon, Ecaterina Avram

"Petru Poni" Institute of Macromolecular Chemistry, Aleea Grigore Ghica Voda 41A, 700487 Iasi, Romania

Received 10 February 2005; accepted 29 September 2005
DOI 10.1002/app.23340
Published online in Wiley InterScience (www.interscience.wiley.com).

ABSTRACT: The conformational behavior and unperturbed dimensions of polysulfone and chloromethylated polysulfone with different degrees of substitution were investigated by viscometry in *N,N*-dimethylformamide; we intended to use these results with more complicated structures with different properties and applications. The effects of concentration and temperature on the coil densities and dimensions and of chlorine content on the unperturbed dimension parameters are discussed. © 2006 Wiley Periodicals, Inc. J Appl Polym Sci 101: 524–531, 2006

Key words: conformational analysis; poly(ether sulfones); viscosity

INTRODUCTION

Polysulfones (PSFs) are a class of polymers that contain sulfone groups and aromatic nuclei and are characterized by good optical properties, thermal and chemical stability, mechanical strength, and resistance to extremes of pH and low creep.[1–3] Chain rigidity is derived from the relatively inflexible and immobile phenyl and SO_2 groups, whereas toughness is derived from the connecting ether oxygen.[4] The chemical modification of PSF, especially the chloromethylation reaction, has been the subject of considerable research interest from both the theoretical and practical points of view, including the production of precursors for functional membranes, coatings, ion-exchange resins, ion-exchange fibers, and selectively permeable films.[2,5,6] Thus, chemical modification is an efficient method for improving the polymer properties. PSFs and chloromethylated polysulfone (CMPSF) have shown many interesting properties; this has led to a wide spectrum of industrial and environmental applications.[7–9] Also, the different components of a block or graft copolymer may segregate in bulk, yielding nanometer-sized patterns or mesophasic structures. There are many applications for the nanodomained solids.[10] Matching the periodicity of the patterns with the wavelength of visible light, researchers have demonstrated that block copolymers, including PSF, function as photonic crystals. Segregated block copolymers, including PSF, have also been used as precursors for the preparation of various nanostructures, including nanospheres, nanofibers, annotates, and thin films containing nanochannels. Thin nanochannels containing films have been used as membranes, pH sensors, and templates for preparing metallic nanorods. Therefore, one of the extremely important roles in PSF applications is played by the control balance between the solution properties of PSF and other chemically modified structures. Thus, for multiple applications, a knowledge of the solution properties before and after the preparation process is necessary.

Previous publications have presented the syntheses[11,12] and some solution properties[13,14] of a series of PSFs. Studies have been carried out on the chloromethylation reaction for the production of soluble chloromethylated polymers with different degrees of substitution (DSs). The purpose of this study was to provide information on the conformational behavior and unperturbed dimensions of PSF and CMPSF for their further utilization in more complicated structures with different destinations.

EXPERIMENTAL

Materials

UDEL-1700 PSF [Union Carbide, Texas City, TX; number-average molecular weight (M_n) = 39,000; weight-average molecular weight/M_n = 1.625] was a commercial product. It was purified by repeated reprecipitation from chloroform and dried for 24 h in vacuo at 40°C before use in the synthesis of CMPSF.

A mixture of commercial paraformaldehyde with an equimolar amount of chlorotrimethylsilane (Me_3SiCl) as a chloromethylation agent and stannic tetrachloride ($SnCl_4$) as a catalyst was used for the chloromethylation reaction of PSF at 50°C. The reaction time was

Correspondence to: S. Ioan (ioan_silvia@yahoo.com).

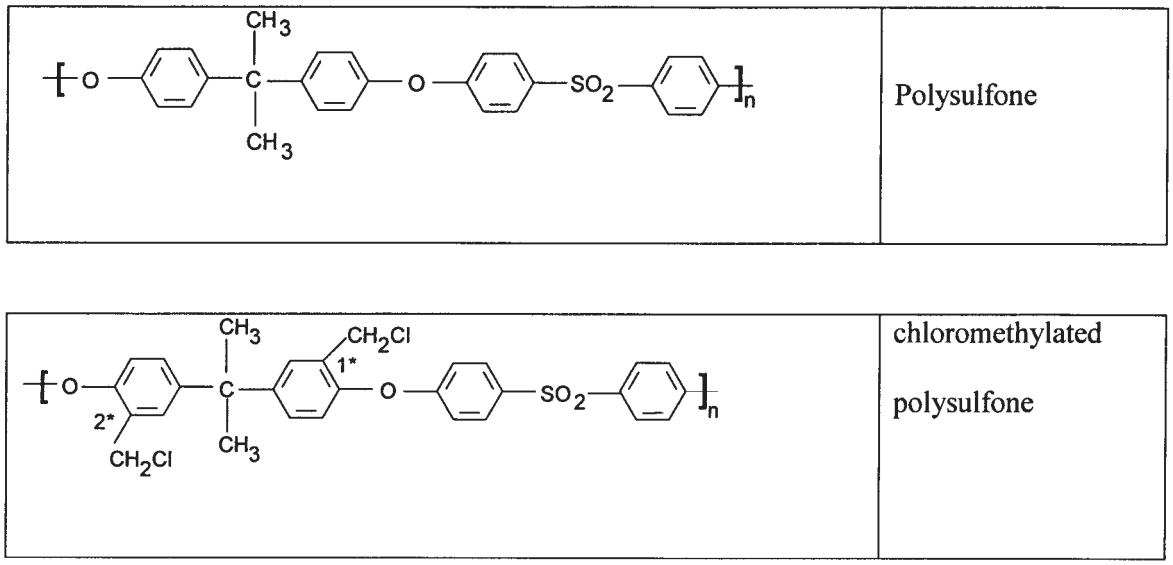

Scheme 1 General structure of PSF and CMPSF.

varied from 24 to 140 h to produce different DSs in the CMPSFs.[12] Finally, the samples were dried in vacuo at 40°C.

The general chemical structures of PSF and CMPSF are presented in Scheme 1.

In the case of PSF, the substitution reaction took place in the beginning in position 1* of the bisphenol ring until the DS was 1 and then took place in position 2* until the DS was 2.

Table I presents values for the content of chlorine, DS, molecular weight of the structural units (m_0), M_n of the CMPSFs determined from the polymerization degree of the PSF (polymerization degree = 90), and m_0's of CMPSFs. Table I also shows the intrinsic viscosity ([η]) determined in *N,N*-dimethylformamide (DMF) at 25°C.

Measurements

Viscosity measurements were carried out in DMF in the 15–45°C temperature range (±0.01°C) on an Ubbelohde suspended-level viscometer (Schott-Gerate GmbH, Mainz, Germany). The kinetic energy corrections were negligible. The flow volume of the used viscometer was above 5 mL, which made drainage errors unimportant. Flow times were obtained with an accuracy of ±0.035% for different measurements of the same samples in DMF at a given temperature. [η]'s were determined by the Huggins[15] and Rao[16] equations, with the latter being only slightly sensitive to the possible errors that may occur in the determination of relative viscosity (η_{rel}):

$$\eta_{sp}/c = [\eta] + k_H[\eta]^2_{Huggins}c \quad (1)$$

$$\frac{1}{2(\eta_{rel}^{1/2} - 1)} = \frac{1}{[\eta]_{Rao}c} - \frac{(a-1)}{2.5} \quad (2)$$

where [η] Huggins is the intrinsic viscosity determined from eq. (1), $[\eta]_{Rao}$ is the intrinsic viscosity determined from eq. (2), η_{sp} is the specific viscosity, k_H is the Huggins constant, c is the concentration of the polymer solution, Φ_m is the maximum volume fraction to which the particles can pack, as expressed by $\Phi_m = ([\eta]/2.5)c_m$, and c_m is a polymer concentration parameter for a given polymer-solvent system, which corresponds to maximum volume fraction to which the particles can pack. Figure 1 shows the representations from which [η]'s were determined for PSF at 15°C: $[\eta]_{Huggins} = 0.373$ and $[\eta]_{Rao} = 0.380$. $[\eta]_{Rao}$ was higher than $[\eta]_{Huggins}$ by about 1.88%. This error was within the limit of the errors given by the methods used to calculate [η].[17] For this reason, the values of [η] used in this work were obtained by the Huggins method.

TABLE I
Content of Chlorine and DS, m_0, M_n, and [η] Values of PSF and CMPSFs in DMF at 25°C

Sample	CI (%)	DS	m_0	M_n	[η] (dL/g)
PSF	0	0.000	442.51	39,000	0.3627
CMPSF1	3.34	0.437	463.68	40,866	0.3929
CMPSF2	8.67	1.231	502.15	44,257	0.4497
CMPSF3	10.53	1.541	517.17	45,580	0.4703
CMPSF4	12.13	1.828	530.83	46,785	0.6970

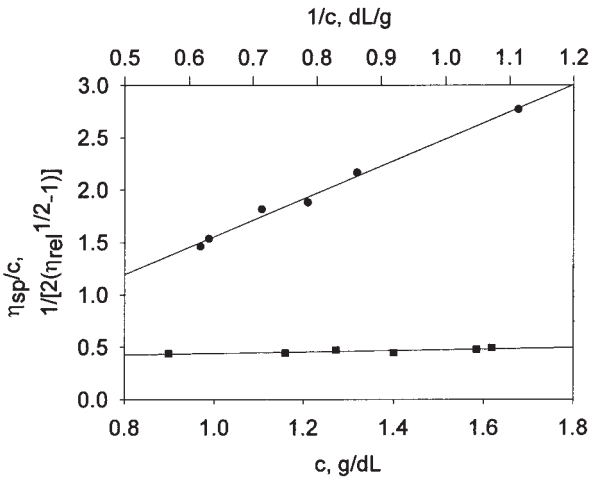

Figure 1 (●) and (■) plots for PSF in DMF at 15°C.

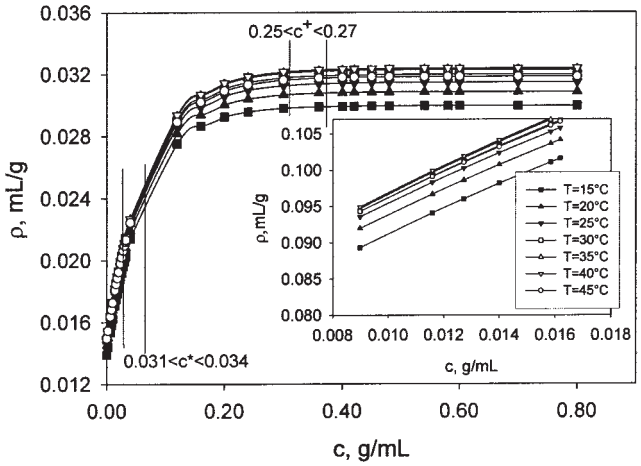

Figure 3 Variation of ρ with concentration for PSF in DMF at different temperatures (*T*s). The small plot corresponds to the experimental data in dilute solution.

RESULTS AND DISCUSSION

Influence of temperature on [η]

Figure 2 shows that [η] decreased with temperature for PSF and the CMPSF2 samples. This variation was obtained for all of the studied samples and is normal for polymers in good solvents.

Coil densities (ρ's) and dimensions in solution

The method of Qian et al.[18] for the determination of [η] in the unperturbed state was used according to eqs. (3)–(6). The unperturbed values obtained from these equations for polystyrene, polyoxyethylene, poly(methyl methacrylate), poly(vinyl chloride), and poly(isobutene) were consistent with the experimental values at θ conditions or with the values calculated according to Mark–Houwink–Sakurada equation at θ conditions. Also, our previous data[19–22] used the viscometric study for the conformational characterization of polyurethanes by this method:

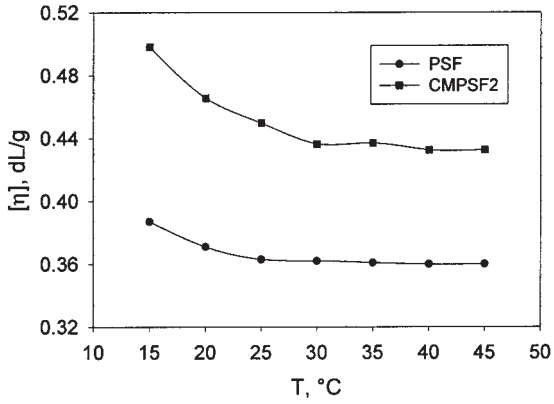

Figure 2 Variation of [η] with temperature for PSF and CMPSF2.

$$[\eta]_\theta = \frac{[\eta]\left[1 - \exp\left(-\frac{c}{c^*}\right)\right]}{\frac{0.77^3\rho}{c^*} - \exp\left(-\frac{c}{c^*}\right)} \tag{3}$$

where $[\eta]_\theta$ is the intrinsic viscosity in unperturbed state, c^* is the critical concentration at which the polymer coils begin to overlap each other, as defined by eq. (4); N_A is Avogadro's number; and ρ is coil density, as approximated by eq. (5) or (6):

$$c^* = \frac{3M}{4\pi N_A R_G^3} = \frac{3\phi'}{4\pi N_A[\eta]} \tag{4}$$

where R_G is the radius of gyration of the polymer molecule in solution, M is the number-average molecular weight, and $\phi' = 3.1 \times 10^{24}$.[19,20]

$$\rho = \frac{c}{\eta_{sp}}(1.25 + 0.5\sqrt{56.4\eta_{sp} + 6.25}) \tag{5}$$

$$\rho = \frac{c^*}{0.77^3\left\{1 + \frac{[\eta] - [\eta]_\theta}{[\eta]_\theta}\left[1 - \exp\left(-\frac{c}{c^*}\right)\right]\right\}} \tag{6}$$

To determine ρ of the PSF and CMPSF chains in solution, eq. (5) was applied. Figures 3 and 4 show the concentration dependence on ρ for PSF and CMPSF2, respectively, in DMF at different temperatures in the dilute range and for a large concentration domain. The small plot corresponds to the experimental data in dilute solution.

The polymer ρ increased with increasing polymer concentration, whereas at a critical concentration (c^+) from the semidilute domain, approximated by

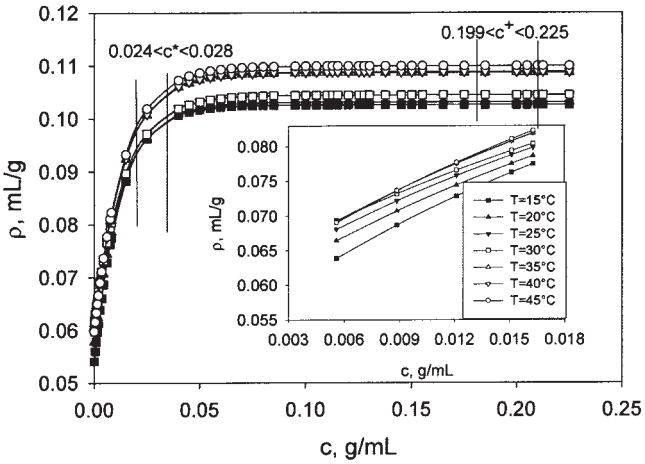

Figure 4 Variation of ρ with concentration for CMPSF2 in DMF at different temperatures (*T*s). The small plot corresponds to the experimental data in dilute solution.

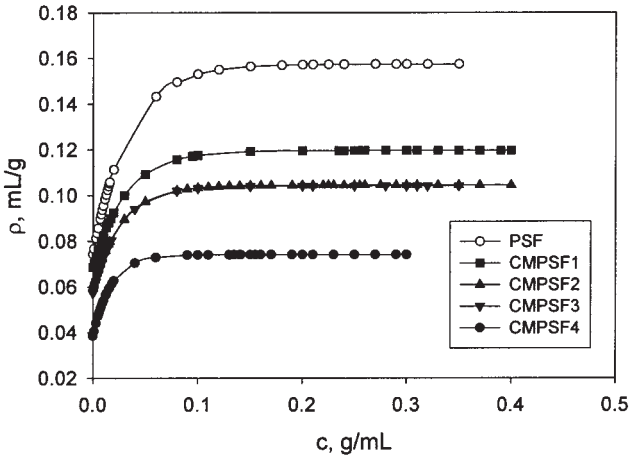

Figure 6 Variation of ρ for a large concentration domain of PSF and CMPSFs in DMF at 25°C.

$c^+ \cong 8c^*$,[23,24] ρ remained constant. Thus, the density at $c \geq c^+$ corresponded to the density in the unperturbed state. The critical concentrations c^* and c^+ are delimited in Figures 3 and 4 for different temperatures. Figures 5 and 6 show the same dependences for all of the studied samples at 25°C for the dilute range and a high domain of concentration, respectively.

ρ in solution was higher for PSF than for CMPSF and decreased with increasing DS.

The modification of ρ was reflected in the variation of R_G with concentration. According to Qian and Rudin,[23,24] the concentration dependence of R_G is calculated with eq. (7):

$$R_G^3 = \frac{3M[\eta]}{3\phi'\left\{1 + \frac{[\eta] - [\eta]_\theta}{[\eta]_\theta}\left[1 - \exp\left(-\frac{c}{c^*}\right)\right]\right\}} \quad (7)$$

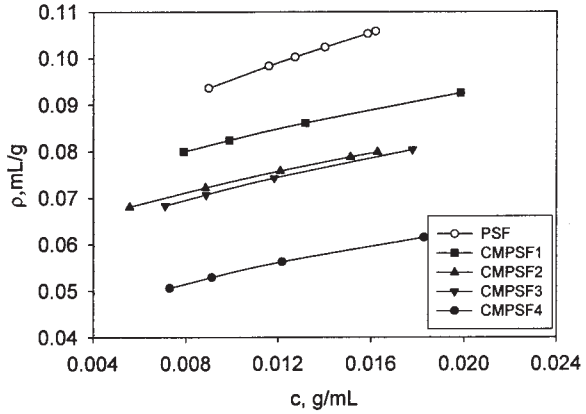

Figure 5 Variation of ρ in dilute solution with concentration for PSF and CMPSFs in DMF at 25°C.

Figures 7–9 plot these dependences for PSF, CMPSF2, and all of the samples from Table I, respectively. R_G values decreased with increasing concentration, whereas at the critical concentration c^+ (identical values with those from Figs. 3 and 4), they shrank to their unperturbed dimensions.

Furthermore, the dimensions in solution were smaller for PSF than for CMPSF and increased with increasing DS. Nevertheless, the ρ's (Fig. 5) and R_G's (Fig. 9) of CMPSF2 and CMPSF3 samples were close. This proximity may have been due to small differences in DS, together with the possible errors in the analytical determination of the chlorine content.

Unperturbed dimension parameters (K_θ's) and steric hindrances (σ's)

In this study, $[\eta]_\theta$ was calculated according to eqs. (3)–(6) with the data of η_{sp}/c at different concentra-

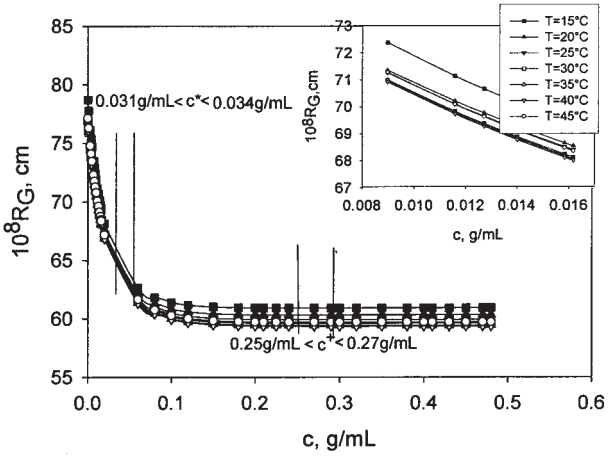

Figure 7 Variation of R_G with concentration for PSF in DMF at different temperatures (*T*s). The small plot corresponds to the experimental data.

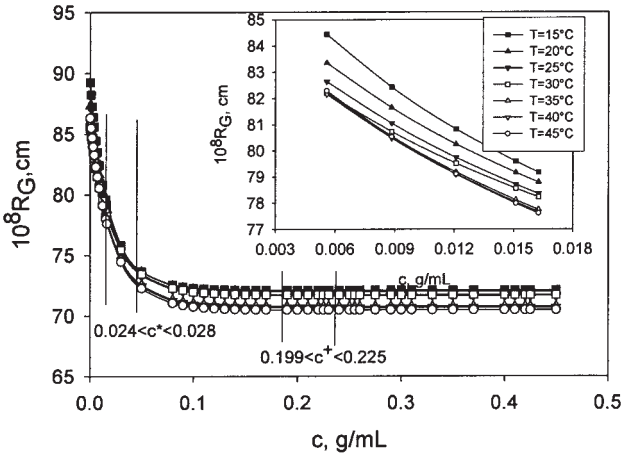

Figure 8 Variation of R_G with concentration for CMPSF2 in DMF at different temperatures (*T*s). The small plot corresponds to the experimental data.

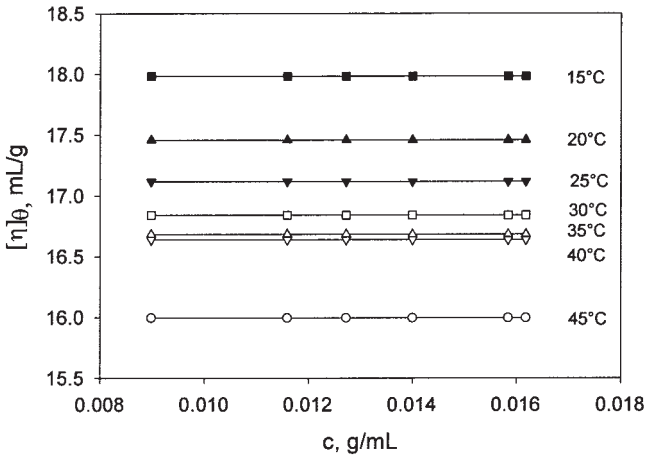

Figure 10 Plot of intrinsic viscosity in unperturbed state versus concentration for PSF at different temperatures calculated according to eq. (3).

tions. The results for PSF and CMPSF at different concentrations and at different temperatures are shown in Figures 10 and 11, respectively. The $[\eta]_\theta$ values were constant for different concentrations, which indicated the viability of eq. (3), but they decreased slightly with increasing temperature.

Figure 12 also presents the $[\eta]_\theta$ values determined for PSF, CMPSF1, CMPSF2, CMPSF3, and CMPSF4 at different concentrations at 25°.

K_θ's, presented in Figure 13, were calculated with eq. (8):

$$[\eta]_\theta = K_\theta M^{1/2} \tag{8}$$

These results seem to indicate that K_θ easily decreased with increasing temperature for all of the studied samples and increased with increasing chlorine content in CMPSF.

The effect of the free rotation around a bond, as a result of σ, was calculated from

$$\sigma = (\langle r_0^2 \rangle / M)^{1/2} / (\langle r_{0f}^2 \rangle / M)^{1/2} \tag{9}$$

where $\langle r_0^2 \rangle^{1/2}$ is the mean-square end-to-end distance in the unperturbed state and $\langle r_{0f}^2 \rangle^{1/2}$ is the mean-square end-to-end distance in the unperturbed state calculated on the assumption of free rotation. $\langle r_0^2 \rangle^{1/2}$ was calculated from Flory–Fox equation [eq. (10)] with K_θ from Figure 13 and the Flory constant in unperturbed state $\phi_0 = 2.87 \times 10^{23}$ g/mol for $[\eta]$ expressed in (mL/g). Figure 13 also presents the results obtained for $(\langle r_0^2 \rangle / M)^{1/2}$ at different temperatures:

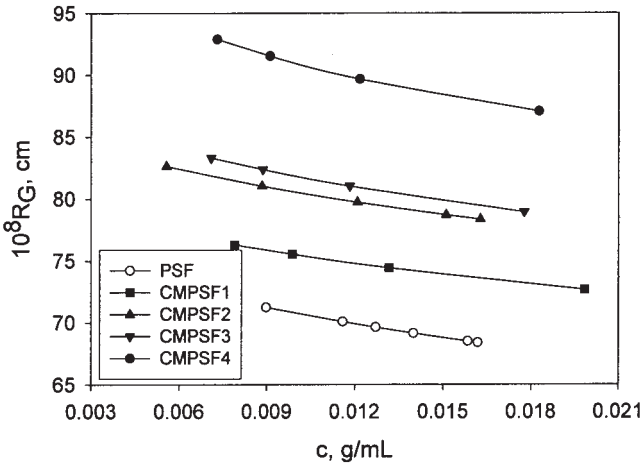

Figure 9 Variation of R_G in dilute solution with concentration for PSF and CMPSFs in DMF at 25°C.

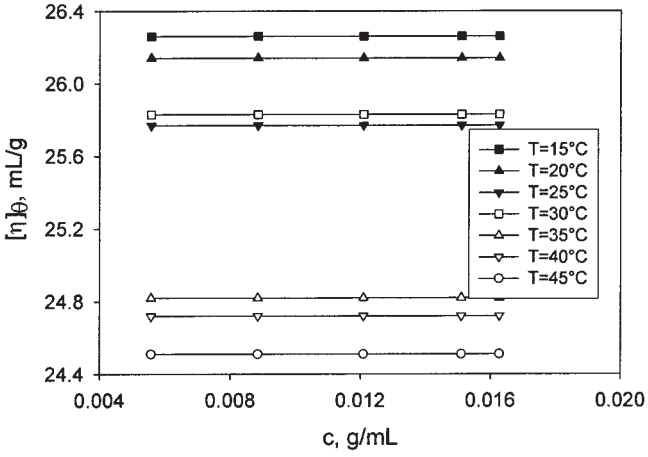

Figure 11 Plot of intrinsic viscosity in unperturbed state versus concentration for CMPSF2 at different temperatures calculated according to eq. (3).

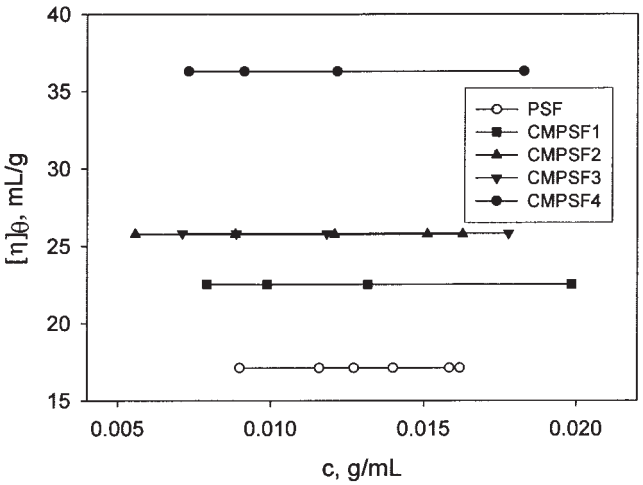

Figure 12 Variation of $[\eta]$ in the unperturbed state with concentration for PSF and CMPSFs in DMF at 25°C.

$$(\langle r_0^2 \rangle / M)^{1/2} = (K_\theta / \phi_0)^{1/3} \tag{10}$$

$(\langle r_0^2 \rangle / M)^{1/2}$ was calculated with the different approximations in the tetrahedral model (Fig. 14).

The approximation of Schulz and Horbach[25] on the polycarbonates, which considered that the chain consists of three valence angles, denoted θ_1, θ_2, and θ_3, and two bond lengths, denoted l and p, with kindred structures to PSF, assumed l = 5.77 Å (corresponding to the bond through the phenylene moiety); p = 1.43 Å (corresponding to the C—O bond); and $\theta_1 = \theta_2$-θ_3 = 109.5 Å.

Thus, $(\langle r_0^2 \rangle / N) = 35.403 \times 10^{-16}$ cm^2 for PSF was obtained from the following relation:

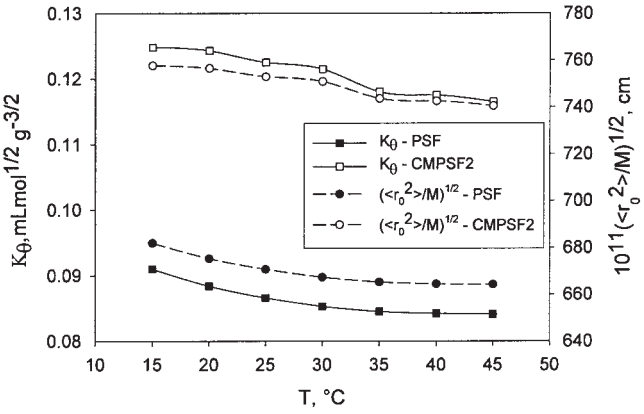

Figure 13 Variation of K_θ the y axis from right with temperature for PSF and CMPSFs in DMF.

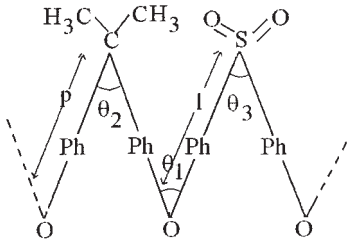

Figure 14 Model chain for PSF.

$$(\langle r_{0f}^2 \rangle / N) = \left(\frac{l^2 + p^2}{2}\right) \times \frac{1 + \cos\theta}{1 - \cos\theta} \tag{11}$$

where N is the total number of links or the number of rotating chain elements ($N = M/m_n$, with m_n = 111 for PSF).

Berry et al.[26] considered the same values for l, p, and θ angles but calculated them from the following relation

$$(\langle r_{0f}^2 \rangle / N) = \left(\frac{l^2 + p^2}{2}\right) \times \left(\frac{1 + \cos(\pi - \theta)}{1 - \cos(\pi - \theta)}\right) \times \left[1 - \frac{(l - p)^2}{(l^2 + p^2)} \times cos(\pi - \theta)\right] \tag{12}$$

This model applied to PSF resulted in $(\langle r_0^2 \rangle / N) = 29.70 \times 10^{-16}$ cm^2.

According to Allen et al.,[27] the PSF chain consists of three valence angles, θ_1 = 123°, θ_2 = 109.5°, and θ_3 = 104°, and two bond lengths, denoted as l = 5.87 Å and p = 5.64 Å. Because θ_2 and θ_3 are very close to the tetrahedral angle 109.5°, the first approximation of Allen et al. considered $\theta_1 = \theta_2 = \theta_3$ = 109.5 Å. Thus, $(\langle r_{0f}^2 \rangle / N) = 66.31 \times 10^{-16}$ cm^2 for PSF at 25°C as calculated by eq. (13):

$$(\langle r_{0f}^2 \rangle / N)^{1/2} = \left[\frac{l^2 + p^2}{2} \times \frac{1 + \cos(\pi - \theta)}{1 - \cos(\pi - \theta)}\right] \times \left[1 - \frac{(l - p)^2}{(l^2 + p^2)} \times \frac{\cos(\pi - \theta)}{1 + \cos^2(\pi - \theta)}\right] \tag{13}$$

In the second approximation of Allen et al.,[27] θ_1 = 123° and $\theta_2 = \theta_3$ = 107°. Thus, the problem becomes one of a molecule consisting of two valence angles and two bond lengths. In this case, $(\langle r_{0f}^2 \rangle / N) = 78.64 \times 10^{-16}$ cm^2 was obtained from the following equation:

TABLE II
m_n, K_θ, $(\langle r_0^2\rangle/M)^{1/2}$, $(\langle r_{0f}^2\rangle/M)^{1/2}$, and σ Values for PSF and CMPSF Samples at 25°C

Sample	m_n	K_θ (mL mol$^{1/2}$/g$^{3/2}$)	$(\langle r_0^2\rangle/M)^{1/2} \times 10^{11}$ (cm)	$(\langle r_{0f}^2\rangle/M)^{1/2} \times 10^{11}$ (cm)	σ
PSF	111	0.0866	670.7	565.0[a]	1.2
				517.3[b]	1.3
				772.9[c]	0.86
				841.7[d]	0.79
CMPSF1	116	0.1114	729.4	552.7[a]	1.3
				506.0[b]	1.4
				756.1[c]	0.96
				823.4[d]	0.89
CMPSF2	126	0.1225	752.9	530.3[a]	1.4
				485.5[b]	1.6
				725.4[c]	1.04
				790.0[d]	0.95
CMPSF3	129	0.1209	749.6	524.1[a]	1.4
				479.9[b]	1.6
				717.0[c]	1.05
				780.8[d]	0.96
CMPSF4	133	0.1677	836.0	516.1[a]	1.6
				472.6[b]	1.8
				706.1[c]	1.2
				769.0[d]	1.1

[a] According to Schulz and Horbach's[25] model.
[b] According to Berry et al.'s[26] model.
[c] According to the first approximation of Allen et al.'s[27] model.
[d] According to the second approximation of Allen et al.'s[27] model.

$$(\langle r_{0f}^2\rangle/N)^{1/2} = \left[\frac{(l^2 + p^2)[1 + \cos(\pi - \theta_1)][1 + \cos(\pi - \theta_2)]}{2[1 - \cos(\pi - \theta_1) \times \cos(\pi - \theta_2)]}\right] \times \left[1 - \frac{(l - p)^2 \times \cos(\pi - \theta_1)[1 - \cos(\pi - \theta_2)]}{(l^2 + p^2)[1 + \cos(\pi - \theta_1) \times \cos(\pi - \theta_2)][1 + \cos(\pi - \theta_1)]}\right] \quad (14)$$

The σ's for PSF and CMPSF with different chlorine contents were calculated in this study by these approximations. Table II presents the $(\langle r_0^2\rangle/M)^{1/2}$ values comparable with the existing literature data for PSF[27] and σ's determined by different approximations. The very small values for σ showed that these polymers possessed very flexible coils and that most of the chain conformations available to the chain with free rotation were accessible to the real chain. These data did not, however, yield information on the height of the rotation barrier, which may be important in other contexts for the designation of a polymer coil as flexible.[28] However, comparative observations of the results from Table II revealed that the rigidity of CMPSF increased with increasing chlorine content. Also, the approximately similar values obtained for σ at different temperatures confirmed the stability of the molecular chains.

Allen et al.[27] mentioned that it was the phenylene ring system that caused the low value of σ, and not the nature of X in the polymers containing —X—Ph—X— links. A significant consequence would appear to be the length of the rigid link and the apparently small energy difference between the various rotational isomers, because it was noticeable that for these polymers, not only was the value of σ very low but also the temperature dependence of chain dimensions. This conclusion was supported by the literature results, which present for aliphatic PSFs with normal main chain linkages consisting of single σ bonds, a σ of 1.71 [corresponding to poly(hexane-1 sulfone)[29,30]] or 2.05 [corresponding to poly(2-methyl-1-pentene-1 sulfone)[29]].

CONCLUSIONS

In this study, information on ρ, R_G at different concentrations and the unperturbed dimension of PSF and CMPSF as a function of temperature were examined, along with their interpretation versus the chlorine content.

The hydrodynamic parameters ($[\eta]$, $[\eta]_\theta$, ρ, and the hydrodynamic volume, V_H) reflected the conformation in solution. Thus, ρ increased with increasing

polymer concentration, whereas from a critical concentration (c^+) in the semidilute domain, it remained constant. ρ at $c \geq c^+$ corresponded to ρ in the unperturbed state.

The modification of ρ was reflected, too, in the variation of R_G with concentration. R_G decreased with increasing concentration, and at the critical concentration c^+, they shrank to their unperturbed dimensions.

K_θ's and $(\langle r_0^2 \rangle / M)^{1/2}$ were comparable with the literature data for PSF, which reflected the influence of the chlorine content in CMPSF. However, chain rigidity derived from the relatively inflexible and immobile phenyl and SO_2 groups was not reflected in the values obtained for σ. The very low values for σ showed that these polymers possessed very flexible coils and that most of the chain conformations available to the chain with free rotation were accessible to the real chain. Thus, these data did not yield information on the height of the barriers to rotation, which may be important in other contexts for the designation of a polymer coil as flexible.

References

1. Barikani, M.; Mehdipour-Ataei, S. J Polym Sci Part A: Polym Chem 2000, 38, 1487.
2. Väisänen, P.; Nyström, M. Acta Polytech Scand 1997, 247, 25.
3. (a) Higuchi, A.; Harashima, M.; Shirano, K.; Hara, M.; Hattori, M.; Imamura, K. J Appl Polym Sci 1988, 36, 1753; (b) Higuchi, A.; Harashima, M.; Shirano, K.; Hara, M.; Hattori, M.; Imamura, K. J Appl Polym Sci 1990, 41, 1973; (c) Higuchi, A.; Harashima, M.; Shirano, K.; Hara, M.; Hattori, M.; Imamura, K. J Appl Polym Sci 1992, 46, 449.
4. Johnson, R. N. In Encyclopedia of Polymer Science and Technology; Herman, F. M.; Norman, G. G.; Bikales, M. N., Eds.; Wiley: New York, 1969; Vol. 11, p 447.
5. Higuchi, A.; Shirano, K.; Harashima, M.; Yoon, B. O.; Hara, M.; Hattori, M.; Imamura, K. Biomaterials 2002, 23, 2659.
6. Tomaszewska, M.; Jarosiewicz, A.; Karakulski, K. Desalination 2002, 146, 319.
7. Savariar, S.; Underwood, G. S.; Dickinson, E. M.; Schielke, P. J.; Hay, A. S. Desalination 2002, 144, 15.
8. Sotiroiu, K.; Pispas, S.; Hadjichristidis, N. Macromol Chem Phys 2004, 205, 55.
9. Ismail, A. F.; Hafiz, W. A. J Sci Technol 2002, 24, 815.
10. Lu, Z.; Liu, G. Macromolecules 2004, 37, 174.
11. Avram, E.; Butuc, E.; Luca, C. J Macromol Sci Pure Appl Chem 1997, 34, 1701.
12. Avram, E. Polym Plast Technol Eng 2001, 40, 275.
13. Ghimici, L.; Avram, E. J Appl Polym Sci 2003, 90, 465.
14. Ioan, S.; Filimon, A.; Avram, E. J Macromol Sci Phys 2005, 44, 129.
15. Huggins, M. L. J Am Chem Soc 1942, 64, 2716.
16. Rao, M. V. S. Polymer 1993, 34, 592.
17. Simionescu, C. I.; Simionescu, B. C.; Neamtu, I.; Ioan, S. Polymer 1987, 28, 165.
18. Qian, J. W.; Wang, M.; Han, D. L.; Cheng, R. S. Eur Polym J 2001, 37, 1403.
19. Ioan, S.; Macocinschi, D.; Lupu, M. J Optoelectron Adv Mater 2003, 5, 563.
20. Ioan, S.; Lupu, M.; Macocinschi, D. High Perf Polym 2003, 15, 319.
21. Ioan, S.; Cojocaaru, I. E.; Macocinschi, D.; Filip, D. High Perf Polym 2004, 16, 123.
22. Ioan, S.; Lupu, M.; Macocinschi, D. Polym Plast Technol Eng 2005, 44, 567.
23. Qian, J. W.; Rudin, A. Eur Polym J 1992, 28, 733.
24. Qian, J. W.; Rudin, A. Eur Polym J 1992, 28, 725.
25. Schulz, G. V.; Horbach, A. Makromol Chem 1959, 29(1/2), 93.
26. Berry, G. C.; Nomura, H.; Mayhan, K. G. J Polym Sci Part A-2: Polym Physics 1967, 5, 1.
27. Allen, G. J.; McAinsh, J.; Strazielle, C. Eur Polym J 1969, 5, 319.
28. Ioan, S.; Bercea, M.; Simionescu, B. C.; Simionescu, C. I. In The Polymeric Materials Encyclopedia: Synthesis, Properties and Applications; Salamone, J. C., Ed.; CRC: Boca Raton, FL, 1996; Vol. 11, p 8417.
29. Bates, T. W.; Biggins, J.; Ivin, K. J. Makromol Chem 1965, 87, 180.
30. Ende, H. A.; Ivin, K. J.; Meyerhoff, G. Polymer 1962, 3, 129.